Regional Extreme Monthly Precipitation Simulated by NARCCAP RCMs

WILLIAM J. GUTOWSKI JR.,[*,+] RAYMOND W. ARRITT,[+] SHO KAWAZOE,[*] DAVID M. FLORY,[*]
EUGENE S. TAKLE,[*,+] SÉBASTIEN BINER,[#] DANIEL CAYA,[#,@] RICHARD G. JONES,[&] RENÉ LAPRISE,[@]
L. RUBY LEUNG,[**] LINDA O. MEARNS,[++] WILFRAN MOUFOUMA-OKIA,[&] ANA M. B. NUNES,[##]
YUN QIAN,[**] JOHN O. ROADS,[##,@@] LISA C. SLOAN,[&&] AND MARK A. SNYDER[&&]

[*] Department of Geological and Atmospheric Sciences, Iowa State University, Ames, Iowa
[+] Department of Agronomy, Iowa State University, Ames, Iowa
[#] Consortium Ouranos, Montreal, Quebec, Canada
[@] Université du Québec à Montréal, Montreal, Quebec, Canada
[&] Met Office, Hadley Centre, Exeter, United Kingdom
[**] Pacific Northwest National Laboratory, Richland, Washington
[++] National Center for Atmospheric Research, Boulder, Colorado
[##] Scripps Institution of Oceanography, University of California, San Diego, La Jolla, California
[&&] University of California, Santa Cruz, Santa Cruz, California

ABSTRACT

This paper analyzes the ability of the North American Regional Climate Change Assessment Program (NARCCAP) ensemble of regional climate models to simulate extreme monthly precipitation and its supporting circulation for regions of North America, comparing 18 years of simulations driven by the National Centers for Environmental Prediction (NCEP)–Department of Energy (DOE) reanalysis with observations. The analysis focuses on the wettest 10% of months during the cold half of the year (October–March), when it is assumed that resolved synoptic circulation governs precipitation. For a coastal California region where the precipitation is largely topographic, the models individually and collectively replicate well the monthly frequency of extremes, the amount of extreme precipitation, and the 500-hPa circulation anomaly associated with the extremes. The models also replicate very well the statistics of the interannual variability of occurrences of extremes. For an interior region containing the upper Mississippi River basin, where precipitation is more dependent on internally generated storms, the models agree with observations in both monthly frequency and magnitude, although not as closely as for coastal California. In addition, simulated circulation anomalies for extreme months are similar to those in observations. Each region has important seasonally varying precipitation processes that govern the occurrence of extremes in the observations, and the models appear to replicate well those variations.

1. Introduction

Precipitation extremes can have substantial impact on human social and economic systems. For this reason, the climatic behavior of precipitation extremes and the ability of models to simulate them attract considerable interest (e.g., Karl et al. 2008). Climate models are used to assess potential changes in extremes decades into the future, for which there is of course no observational verification. One way of increasing confidence in such projections is to show that climate models can reproduce climatological behavior of observed extremes when simulating contemporary climate and that they simultaneously produce the observed environment supporting the extremes (e.g., Gutowski et al. 2008a,b).

Here we provide such an analysis for simulated extremes in monthly precipitation. Extended periods of substantial precipitation represented by monthly extremes can produce widespread episodes of flooding (e.g., Kunkel et al. 1994). We focus on simulations of contemporary climate produced by a set of regional climate models (RCMs) that simulated a common period and domain for the North American Regional Climate Change Assessment Program (NARCCAP) (Mearns et al.

[@@] Deceased.

Corresponding author address: William J. Gutowski Jr., 3021 Agronomy Hall, Iowa State University, Ames, IA 50011.
E-mail: gutowski@iastate.edu

2009). One of NARCCAP's goals is to use an ensemble of RCMs to project statistical properties of regional climate changes for a number of fields. The analysis here focuses on the capability of the ensemble to simulate climatic properties of observed monthly precipitation extremes, including their supporting environment, in order to help establish the degree of confidence one might have in projections of climate change the RCMs are producing for the NARCCAP archive (Mearns et al. 2009).

2. Observations, simulations, and analysis methods

a. Observations

The analysis uses the University of Washington's (UW's) gridded precipitation (Maurer et al. 2002). The dataset uses the Parameter-Elevation Regressions on Independent Slopes Model (PRISM; Daly et al. 1994) corrections for systematic elevation effects on precipitation climatology and provides observation-based precipitation on an eighth-degree grid that covers all of the contiguous United States. This precipitation dataset in the NetCDF format covers the period 1950–99.

We use the monthly circulation associated with observed extreme precipitation as our basis for determining the environment conducive to the extremes. For this part of the analysis, we use 500-hPa geopotential heights from the North American Regional Reanalysis (NARR; Mesinger et al. 2006). The analysis focuses on height anomalies, computed as departures from the 1982–99 average. This period coincides with the period when both observed and simulated precipitation data are available.

b. Simulations

Model output comes from six regional climate models that simulated the period 1979–2004 for NARCCAP (Mearns et al. 2009): the Canadian Regional Climate Model version 4 (designated CRCM in the NARCCAP archive), the Hadley Centre Regional Model version 3 (HadRM3; HRM3 in the archive), the National Center for Atmospheric Research (NCAR) Weather Research and Forecasting Model (WRF; WRFP in the archive), the fifth-generation Pennsylvania State University–NCAR Mesoscale Model (MM5; MM5I in the archive), the International Centre for Theoretical Physics Regional Climate Model version 3 (RegCM3; RCM3 in the archive), and the Experimental Climate Prediction Center's Regional Spectral Model (ECPC in the archive). Details of each model's structure appear in Mearns et al. (2009) and references therein (see also http://narccap.ucar.edu). RCM boundary conditions came from the reanalysis (Kanamitsu et al. 2002) produced by the National Centers for Environmental Prediction (NCEP) and the U.S. Department of Energy (DOE). The models all used
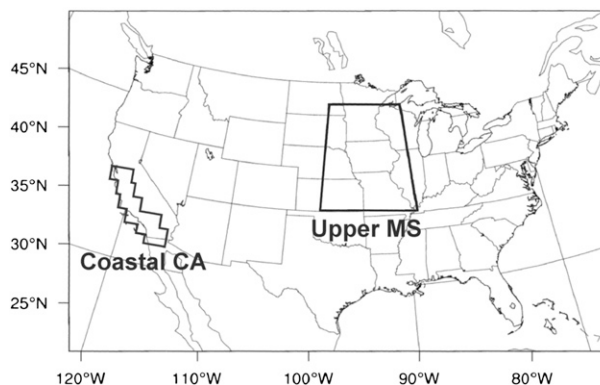

FIG. 1. Region covered by each of the NARCCAP models, along with the two analysis regions: coastal California (Coastal CA) and the upper Mississippi River basin (Upper MS).

approximately half-degree resolution to simulate the region shown in Fig. 1 for the period 1979–2004. Except for the northern side, the boundaries in Fig. 1 correspond roughly with the boundaries of each model's region that was interior to its outer frame where lateral boundary conditions were ingested. On the northern side, the interior region of each model extended into the northern Canadian territories.

c. Analyses

We consider the period 1982–99, discarding the years 1979–81 from the simulations to cover model spinup and ending in the final year of the UW dataset. Because we are working with extremes, we adopted a relatively conservative spinup period to ensure that the models' water cycles were adequately spun up. Our analyses focus on the cold half of the year (October–March) under the assumption that synoptic dynamics are more likely to play a role in producing precipitation during this part of the year compared to the warm half, when smaller-scale convective events may be more important. For synoptic events, the model should resolve the relevant circulation, which it may not be able to do as well for convection-dominated events. We examine monthly precipitation for two subregions in Fig. 1: a coastal California (Coastal CA) region and an upper Mississippi River basin (Upper MS) region. Both regions have an annual maximum in net precipitation (precipitation − evaporation), and hence an accumulation of surface and subsurface water, during the cold half of the year (Gutowski et al. 1997; Hamlet et al. 2007; Tang et al. 2010).

For both Coastal CA and Upper MS, we compute region-averaged precipitation by averaging monthly precipitation over all grid points that fall in the region. We then rank the region's monthly precipitation for the observations and for each model and perform further analysis
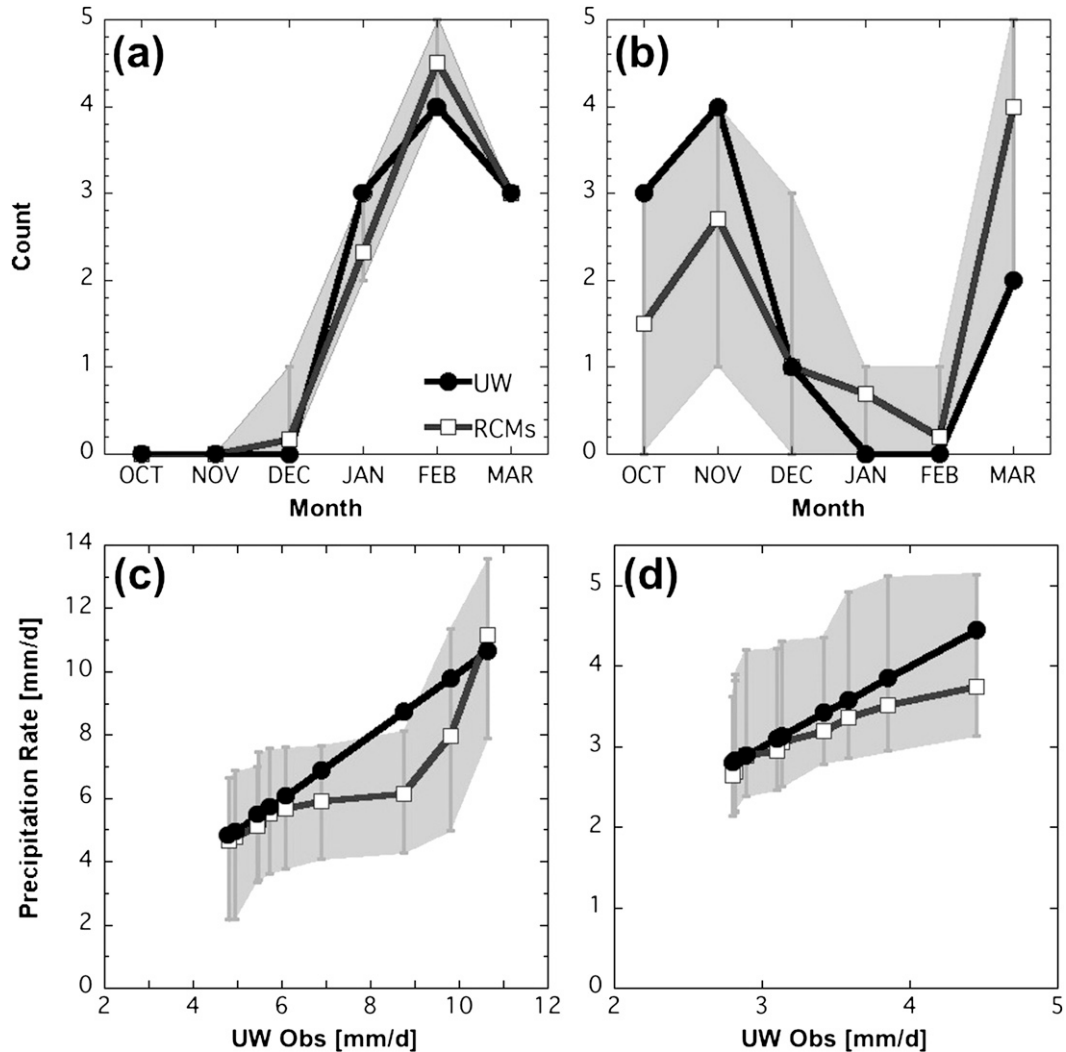
FIG. 2. Frequency distribution of extreme precipitation months in the observations (UW) and in the NARCCAP RCMs for the (a) Coastal CA and (b) Upper MS regions, and ranked extreme monthly precipitation in the observations and the RCMs plotted against the ranked observations for the (c) Coastal CA and (d) Upper MS regions. The RCM curve is the average among corresponding values from the six RCMs. The shaded regions and I-bars show the spread of values among the RCMs.

using the 10 months from each source with the greatest precipitation. For our 18-yr analysis period focusing on the cold half of the year, the 10 extreme months are essentially the upper 10% of monthly precipitation. Note that the months in the top 10% are not necessarily the same in the observations and each model, although there is considerable overlap.

3. Extreme monthly precipitation

Figure 2 shows the seasonal frequency distribution for the extreme-precipitation months for the models versus observations. In both regions, there is substantial seasonal variation in the observed frequency distribution,

producing a clear feature for the models to replicate. For Coastal CA, the ensemble average frequency distribution replicates well the observed frequency distribution, as differences between the two for any month are always much smaller than the range of frequency variation through the season. Moreover, each individual model reproduces the seasonal variation well because the spread in frequency distribution among the models is also relatively small. Despite the narrow spread, the frequency range among the models encompasses the observed frequency in each month. For Upper MS, the models show greater spread in their individual frequency distributions, and so overall agreement with the observed frequency distribution is not as strong as for Coastal CA. The models'

ensemble average still captures the primary features of the seasonal variation, with maxima in November and March and a low-frequency period in January and February.

Figure 2 also shows the ranked precipitation in the models plotted against the ranked precipitation in the observations. The models collectively simulate fairly well the magnitude of the extreme precipitation. For Coastal CA, the threshold for the top 10% in the observations is 4.8 mm day^{-1}; averaged among the models it is 4.7 mm day^{-1} or 2% less. The average precipitation amount among the top 10% of observed months is 6.9 mm day^{-1}, whereas the models' ensemble average of the top 10% months is 6.2 mm day^{-1}, or 10% less. The models tend to simulate less well the precipitation magnitudes of the more extreme months. For example, the average precipitation among the top 5% months in the observations is 8.4 mm day^{-1}, but the models' ensemble average among the top 5% is only 7.4 mm day^{-1}, or 12% less.

For Upper MS, the top 10% threshold is 2.8 mm day^{-1}, and averaged among the models it is 2.6 mm day^{-1}, or 7% less. The average precipitation among the top 10% of observed months is 3.3 mm day^{-1}, and among the models it is 3.1 mm day^{-1}, or 6% less. Again, the models tend to simulate less well the more extreme precipitation amounts. For just the top 5% months, the observed average is 3.7 mm day^{-1}, and the models' ensemble average is 3.4 mm day^{-1}, or 8% less.

Finally, the models tend to produce features of interannual variability seen in the observations. For Coastal CA, 59 out of the 60 extremes (98%) in the models occur in a cold season when at least one observed extreme occurs. The observed top 10% months occur in 8 of the 18 cold seasons, so if the 60 model extremes were randomly distributed among the years, only 27 of the extremes (45%) would occur, on average, in the same year as an observed extreme. For Upper MS, 46 of 60 extremes (77%) occur in a cold season with at least one observed extreme. The observed top 10% months occur in 10 of the 18 cold seasons, so randomly distributed extremes would occur, on average, 33 times (56%) in a cold season with an observed extreme. For both regions, the degree of agreement between models and observations for cold seasons with extremes is substantially higher than what would occur by random chance.

4. Supporting circulation

The monthly precipitation extremes are presumably linked to atmospheric circulation. We evaluate monthly 500-hPa height anomalies as an indicator of the circulation features leading to extremes in the observations and the models. For the observed extremes and for each

model's extremes, we compute the composite anomaly produced by averaging 500-hPa height anomalies for the months with the top 10% of precipitation amounts. The composite anomalies appear in Fig. 3 (Coastal CA) and Fig. 4 (Upper MS). The circulation anomaly for each individual month is similar to its corresponding composite, so each composite is representative of all its contributing anomalies.

For Coastal CA, a distinctive feature in the composites for the observations and for each model is a band of low height anomalies extending from the Pacific Ocean to the U.S. West Coast. The mean circulation around such an anomaly would promote flow from the ocean toward the coastal and interior mountains of southern California, features that are resolved by the models and that would produce topographic precipitation. The models all show agreement with observations on the supporting circulation anomaly. This feature contrasts with the composite anomalies for the bottom 10% of precipitation amounts, which in each case has a high height anomaly along the West Coast (not shown). Figure 3 also shows the average precipitation for the top 10% extremes. The amount of precipitation varies approximately with the amplitude of the 500-hPa height anomalies along the West Coast and eastern Pacific. This might be expected as much of the cold season precipitation is produced by westerly winds blowing against the orography of California.

For Upper MS, the agreement among models, and with the observed anomalies, is not as strong as for Coastal CA, but nonetheless some common features emerge. All have a low height anomaly in the western half of the United States and a high anomaly to the east or northeast. A major source of moisture for precipitation in the central United States is the Gulf of Mexico. The anomaly circulation patterns promote the flow of moisture from the Gulf to the Upper MS region (Arritt et al. 1997). As with Coastal CA, the bottom 10% months have composite 500-hPa height anomalies (not shown) that are roughly the opposite of those in Fig. 3: an area of high heights in the western United States and low heights to the east or southeast. Figure 4 also shows the average precipitation for the top 10% extremes. Here, there is no clear association between the amount of precipitation and the amplitude of the 500-hPa height anomalies. In contrast to Coastal CA, the cold season precipitation is more complex than simple orographic uplift and depends on factors such as storm growth and decay in the region, so the lack of an association with the amplitude of anomalies is perhaps not surprising.

Two of the models (ECPC and CRCM) ingest large-scale flow information in their interiors in addition to lateral boundary conditions, but examination of Figs. 3
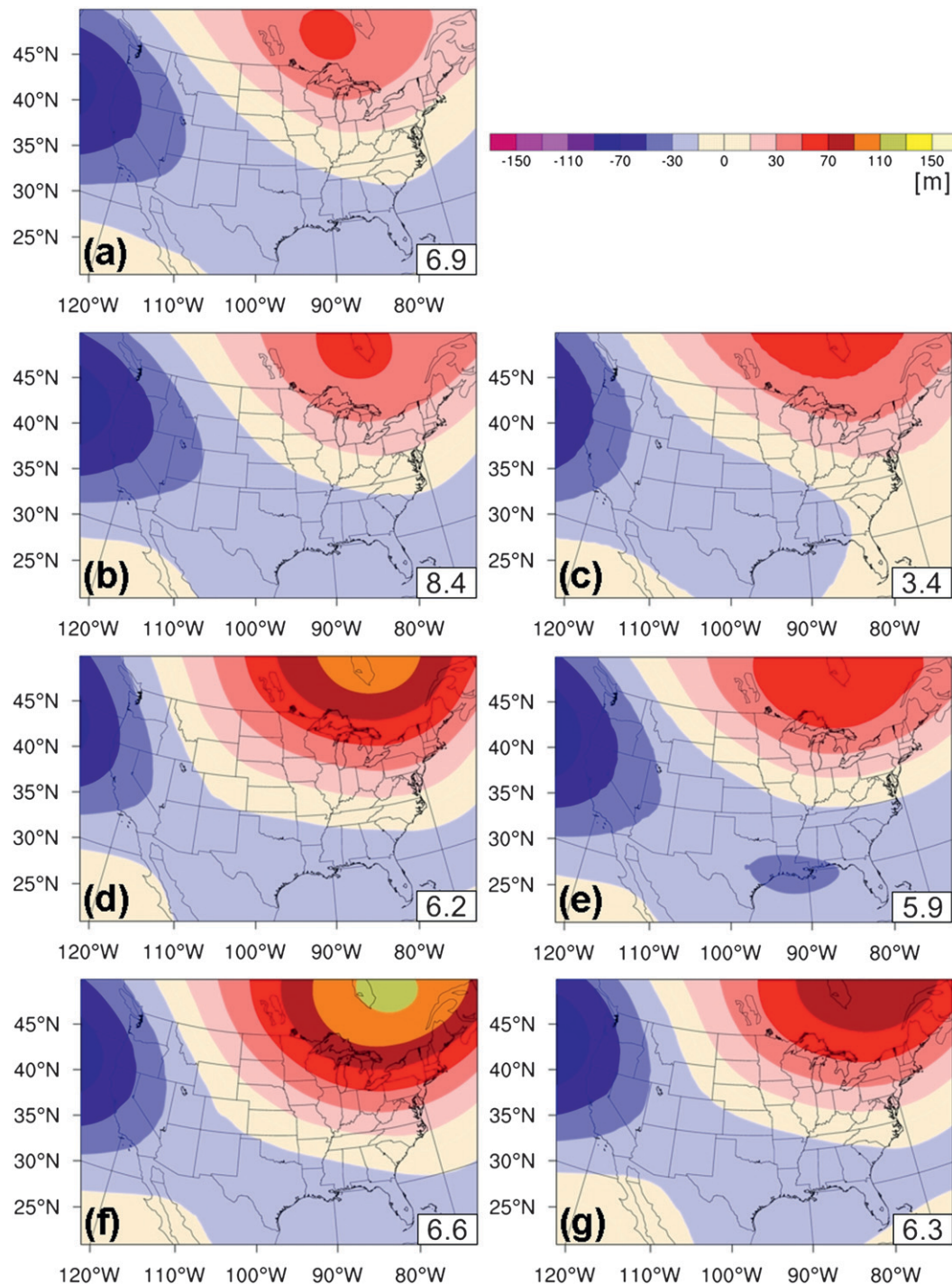
FIG. 3. Composite 500-hPa height anomalies for top 10% of Coastal CA monthly precipitation extremes: (a) NARR, (b) ECPC, (c) HRM3, (d) MM5I, (e) CRCM, (f) RCM3, and (g) WRFP. Contour scale for all plots is in the upper right. Insets on the lower right of each panel give the average precipitation for the top 10% extremes, with UW precipitation in (a). Contours are in meters, and precipitation is in mm day^{-1}.
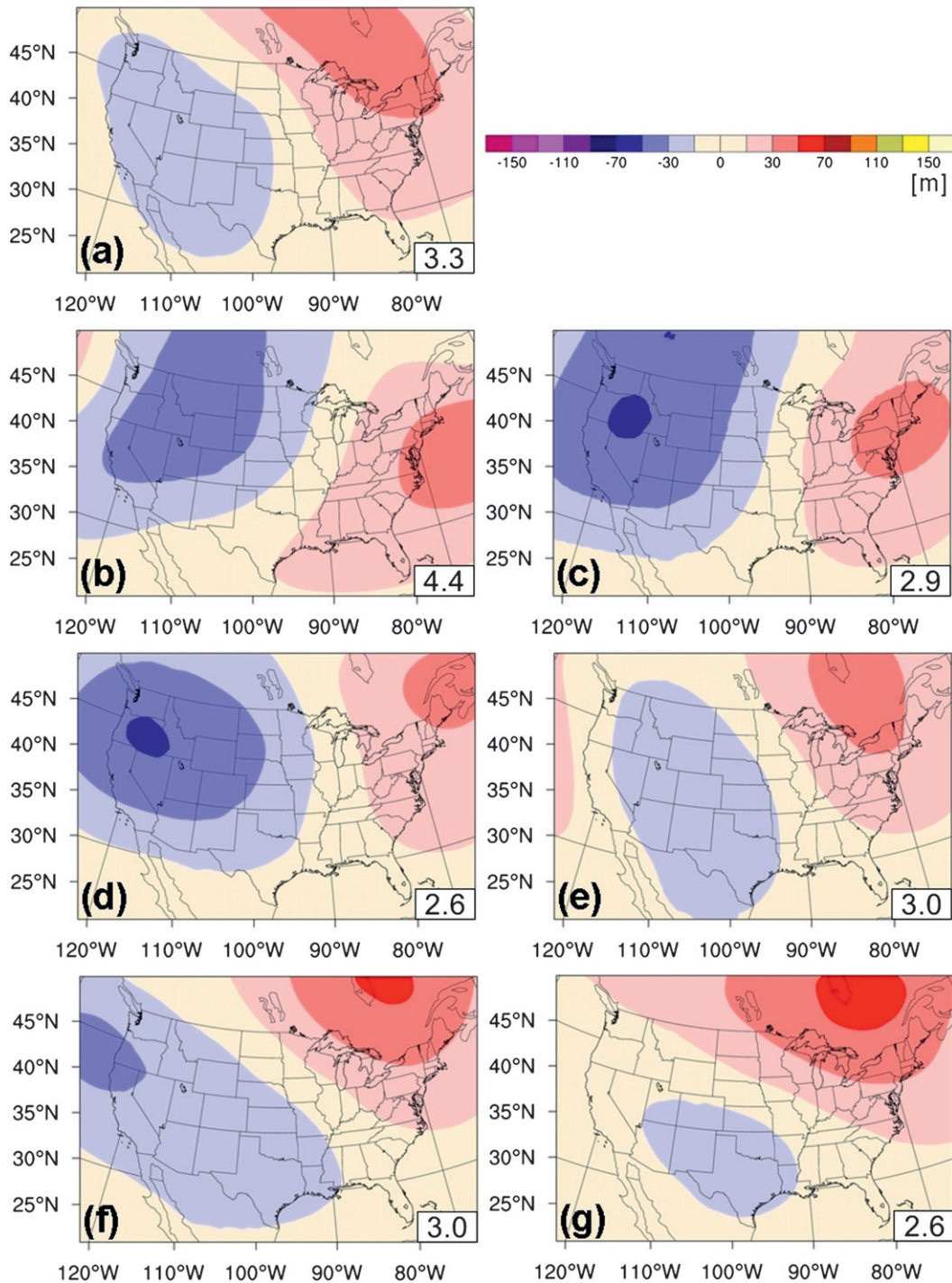
FIG. 4. As in Fig. 3, but for the top 10% of Upper MS monthly precipitation extremes.

and 4 shows that this feature does not guarantee closer agreement in anomaly circulation patterns with the re-analysis. As noted earlier, the top 10% months are not necessarily the same in the observations and each model, although there is considerable overlap. Thus differences in precipitation simulation that yield differences in

which months are deemed extreme can also affect de-tails of the resulting anomaly patterns.

5. Conclusions

For the two regions examined here, the ensemble of NARCCAP models reproduce well several features of

observed extreme monthly precipitation, defined as the top 10% of monthly precipitation in the cold half of the year (March–October) for the period 1982–99. Collectively, the models reproduce well the seasonal variation and interannual variability of the timing of extremes. They also reproduce to within 10% the average magnitude of the top 10% of monthly extremes. One reason for the fairly good behavior of the ensemble for coastal California is that the models also reproduce well the monthly circulation anomalies for the extreme months, as measured by the composite 500-hPa anomalies. The models' 500-hPa anomalies for extreme months in the Upper Mississippi Basin do not match the corresponding reanalysis anomalies as well as they do for coastal California. However, they do all reproduce one key factor: the anomaly circulations promote moisture flow into the center of the United States from the Gulf of Mexico.

Better agreement with observations occurs for the coastal California region, which might be expected, as it is nearer to the inflow boundary. Also, the precipitation process for the extremes appears to require simply moist air flowing upward over topography. In the central United States, replication depends more strongly on the ability of the models to produce synoptic storm climatology similar to the observed climatology, which the models do to some extent by virtue of their similar extreme precipitation and circulation anomalies.

Another key factor for the success of the ensemble in these two regions is that both regions have substantial seasonal variation in the frequency of extremes. The behavior suggests that each region has important seasonally varying precipitation processes that govern the occurrence of extremes in the observations and that provide a strong signal of seasonal change for the models to capture. For the upper Mississippi basin, this may be simply the specified seasonal temperature variation in the Gulf of Mexico, which allows more moisture transport into the central United States when it is relatively warm in autumn and less during the colder winter months. For coastal California, the behavior may be linked to the seasonal movement of the climatological jet stream.

REFERENCES

Arritt, R. W., T. D. Rink, M. Segal, D. P. Todey, C. A. Clark, M. J. Mitchell, and K. M. Labas, 1997: The Great Plains low-level jet during the warm season of 1993. *Mon. Wea. Rev.,* **125,** 2176–2192.

Daly, C., R. P. Neilson, and D. L. Phillips, 1994: A statistical–topographic model for mapping climatological precipitation over mountainous terrain. *J. Appl. Meteor.,* **33,** 140–158.

Gutowski, W. J., Y. Chen, and Z. Ötles, 1997: Atmospheric water vapor transport in NCEP–NCAR reanalyses: Comparison with river discharge in the central United States. *Bull. Amer. Meteor. Soc.,* **78,** 1957–1969.

——, and Coauthors, 2008a: Causes of observed changes in extremes and projections of future changes. *Weather and Climate Extremes in a Changing Climate—Regions of Focus: North America, Hawaii, Caribbean, and U.S. Pacific Islands,* T. R. Karl et al., Eds., National Climatic Data Center, 81–116.

——, S. S. Willis, J. C. Patton, B. R. J. Schwedler, R. W. Arritt, and E. S. Takle, 2008b: Changes in extreme, cold-season synoptic precipitation events under global warming. *Geophys. Res. Lett.,* **35,** L20710, doi:10.1029/2008GL035516.

Hamlet, A. F., P. W. Mote, M. P. Clark, and D. P. Lettenmaier, 2007: Twentieth-century trends in runoff, evapotranspiration, and soil moisture in the western United States. *J. Climate,* **20,** 1468–1486.

Kanamitsu, M., W. Ebisuzaki, J. Woollen, S. K. Yang, J. J. Hnilo, M. Fiorino, and G. L. Potter, 2002: NCEP/DOE AMIP-II reanalysis (R-2). *Bull. Amer. Meteor. Soc.,* **83,** 1631–1643.

Karl, T. R., G. A. Meehl, C. D. Miller, S. J. Hassol, A. M. Waple, and W. L. Murray, Eds., 2008: *Weather and Climate Extremes in a Changing Climate—Regions of Focus: North America, Hawaii, Caribbean, and U.S. Pacific Islands.* National Climatic Data Center, 164 pp. [Available online at http://downloads.climatescience.gov/sap/sap3-3/sap3-3-final-all.pdf.]

Kunkel, K. E., S. A. Changnon, and J. R. Angel, 1994: Climatic aspects of the 1993 Upper Mississippi River Basin flood. *Bull. Amer. Meteor. Soc.,* **75,** 811–822.

Maurer, E. P., A. W. Wood, J. C. Adam, D. P. Lettenmaier, and B. Nijssen, 2002: A long-term hydrologically based dataset of land surface fluxes and states for the conterminous United States. *J. Climate,* **15,** 3237–3251.

Mearns, L. O., W. J. Gutowski, R. Jones, L.-Y. Leung, S. McGinnis, A. M. B. Nunes, and Y. Qian, 2009: A regional climate change assessment program for North America. *Eos, Trans. Amer. Geophys. Union,* **90,** 311–312.

Mesinger, F., and Coauthors, 2006: North American Regional Reanalysis. *Bull. Amer. Meteor. Soc.,* **87,** 343–360.

Tang, Q., H. Gao, P. Yeh, T. Oki, F. Su, and D. P. Lettenmaier, 2010: Dynamics of terrestrial water storage change from satellite and surface observations and modeling. *J. Hydrometeor.,* **11,** 156–170.